CANCOM2024 – CANADIAN INTERNATIONAL CONFERENCE ON COMPOSITE MATERIALS

TRANSIENT TRANSVERSE DEFORMATION OF THERMOPLASTIC COMPOSITE TAPE IN AUTOMATED FIBER PLACEMENT

Fereidouni, M. [1, 2, *] and Hoa, S.V. [1, 2]

[1] Concordia Center for Composites
Department of Mechanical, Industrial and Aerospace Engineering, Concordia University
Montreal, Quebec, Canada

[2] Research Center for High-Performance Polymer and Composite System (CREPEC)
Montreal, Quebec, Canada

* Corresponding author (mahmoud.fereidouni@mail.concordia.ca)

Keywords: *Transverse Squeeze Flow, Thermoplastic Composites, Automated Fiber Placement*

ABSTRACT

In-situ consolidation of thermoplastic composites using automated fiber placement (AFP) has attracted substantial interests for manufacturing of geometrically complex or variable stiffness composite structures out-of-autoclave. Outstanding AFP capabilities are accompanied by the emergence of diverse defects, including gaps and overlaps between adjacent tapes in laminate. The deformation of material and the final width of tape after the AFP consolidation dictates the size of gaps or overlaps. Transverse squeeze flow of CF/PEEK tape under compaction force of AFP equipment has been measured experimentally and a model was developed to analyze the deformation of tape. Equations of motion were expressed based on two-dimensional creeping flow for transversely isotropic molten composite tape. Strain rate dependent viscosity of material under rapid deformation was captured using power-law relation and transverse wall slippage at top and bottom interfaces was included using Navier slip condition. The results for final dimensions of processed tape were obtained using the model and compared against experimental measurements for samples made using hot gas torch assisted AFP machine under different compaction forces and temperatures.

1 INTRODUCTION

Conspicuous transverse squeezing of molten thermoplastic composite tapes under compaction force of automated fiber placement head is one of the major contributing factors to the gap and overlaps of adjacent bands within a ply, which can compromise mechanical performance of the final composite [1]. Agarwal [2] experimentally studied the deformation of CF/PAEK composite tapes in-situ consolidated by flashlamp-assisted AFP equipment and showed that the variations in process parameters resulted in increase of width ranging from 5% to 13%. In another experimental study by Oromiehie *et al.* [3] on in-situ consolidated width of CF/PEEK tape by hard roller, increases within the range of 12% to 70% have been reported by changing basic process parameters. The final width of consolidated tape is a function of various parameters including material properties (e.g., viscosity, level of non-Newtonian behavior), tape cross-sectional geometry (e.g., width and thickness), process parameters (e.g., nip point temperature, layup velocity, compaction force), placement head configuration (e.g., hard or soft roller), tribology of interacting surfaces (e.g., friction between tape and substrate or tape and roller). A theoretical model for deformation of molten thermoplastic tape may assist in gaining insight into the direct effect of each parameter. This work aims to propose a model to predict the final cross-sectional shape of tape with little computational costs. Equations of fluid motion are developed for two-dimensional incompressible flow with Power law viscosity. Navier slip boundary condition is employed for strong transverse wall slippage. The integration of stress-strain-rate equations with respect to space parameters and time lead to relationship between process parameters and final width of consolidated tape.

2 SQUEEZE FLOW MODELING

The stress tensor for two-dimensional incompressible flow with non-Newtonian Power law behavior can be shown as a function of hydrostatic pressure and strain rates [4]:

$$\begin{bmatrix}\sigma_{xx} & \sigma_{xy}\\ \sigma_{yx} & \sigma_{yy}\end{bmatrix} = -p\begin{bmatrix}1 & 0\\ 0 & 1\end{bmatrix} + m\left(4\dot{\varepsilon}_{xx}{}^{2} + \dot{\gamma}_{xy}{}^{2}\right)^{(n-1)/2}\begin{bmatrix}2\dot{\varepsilon}_{xx} & \dot{\gamma}_{xy}\\ \dot{\gamma}_{xy} & -2\dot{\varepsilon}_{xx}\end{bmatrix} \tag{1}$$

The coefficient of the second matrix on the right side of the equation is Power law viscosity expression incorporating both shear strain rate ($\dot{\gamma}_{xy}$) and elongational strain rate ($\dot{\varepsilon}_{xx}$) effects, wherein *n* and *m* are power-law index and consistency parameter, respectively. Subsequently, the balance of stresses can be also derived based on Cauchy momentum equation with neglecting the inertial terms and body forces due to insignificant order of magnitude:

$$\frac{\partial\sigma_{xx}}{\partial x} + \frac{\partial\sigma_{yx}}{\partial y} = 0 \quad \text{(a)} \qquad\qquad \frac{\partial\sigma_{yx}}{\partial x} + \frac{\partial\sigma_{yy}}{\partial y} = 0 \quad \text{(b)} \tag{2}$$

The viscous deformation of fiber-reinforced thermoplastic composite tape as highly anisotropic fluid is confined to transverse flow as reinforcing fibers restrict the extensional flow along fibers. Therefore, the process modelling can be streamlined into assessment of the cross-sectional deformation of composite tape under compaction roller as a two-dimensional flow over time as shown in Figure 1. Fiber-matrix mixture is theoretically assessed as a homogeneous fluid, whose equivalent properties (specifically *m* and *n* parameters) can be taken from available experimental data on rheological characterization.

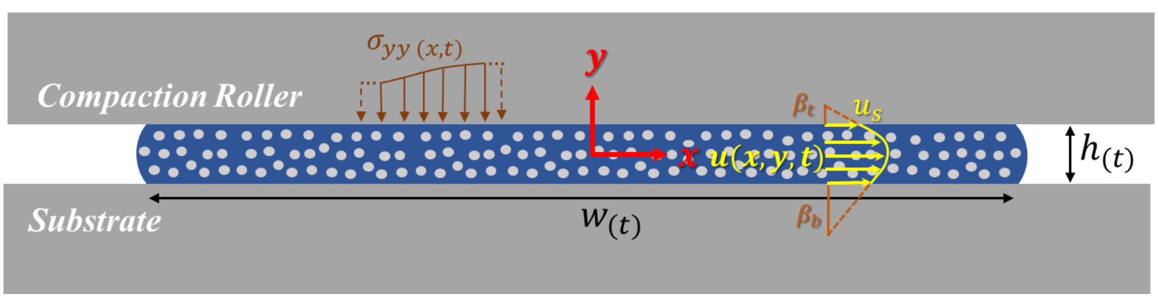

Figure 1. Cross-sectional view of incoming tape being squeezed between substrate and compaction roller.

As shown, *w* and *h* denote instantaneous width and thickness of tape. Meanwhile, *x* and *y* axes are oriented along width and thickness, respectively, and the origin of coordinate system lies on the centroid of the tape cross-section. Finally, *u* and *v* show fluid velocity components along the *x* and *y* axes, respectively.

2.1 Imperfect Slip Condition

Imperfect slip condition is proposed to incorporate the effect of friction at interface (wall) on deformation of tape. Firstly, according to Navier-slip relation [5]:

$$u_{ws} = \beta \frac{du}{dy}|_{wall} \tag{3}$$

Where u_{ws} is slip velocity (fluid tangential velocity with respect to the wall) and β is a constant named slip length (See Figure 1). In the development of imperfect slip squeeze model, the elongational flow is assumed to be dominant. In simple terms, frictional force is small enough compared with compaction force so that $\dot{\gamma}_{xy} \ll \dot{\varepsilon}_{xx}$. With this and attention to Equation 1:

$$\sigma_{xy} = \tau_{xy} = 2^{n-1}\, m\, \dot{\varepsilon}_{xx}{}^{n-1}\, \dot{\gamma}_{xy} \tag{4}$$

By substituting (3) in (4), shear stress at fluid-solid interface will be:

$$\tau_{xy}\,|_{y=\frac{h}{2},-\frac{h}{2}} = 2^{n-1}\, m\, \dot{\varepsilon}_{xx}{}^{n-1}\, \frac{u_{ws}}{\beta} \tag{5}$$

Since $\dot{\gamma}_{xy} \ll \dot{\varepsilon}_{xx}$ ($\frac{du}{dy}$ being relatively small), u can be considered constant across y for a given x. Also:

$$u_{ws} \approx u\,|_{x=c} \tag{6}$$

Additionally, the continuity equation for an instantaneous rectangular control volume (width and height extending from 0 to x and from -h/2 to h/2 respectively) lead to:

$$\dot{h}x = -uh \tag{7}$$

The implementation of (6) and (7) into (5) would result in:

$$\tau_{xy}\,|_{y=\frac{h}{2},-\frac{h}{2}} = 2^{n-1}\, m\, \dot{\varepsilon}_{xx}{}^{n-1}\, \frac{-\dot{h}x}{h\beta} \tag{8}$$

Or:

$$\tau_{xy}\,|_{y=\frac{h}{2},-\frac{h}{2}} = 2^{n-1}\, m\, (\frac{\dot{w}}{w})^{n-1}\, \frac{\dot{w}x}{w\beta} = 2^{n-1}\frac{m}{\beta}\,(\frac{\dot{w}}{w})^{n}\, x \tag{9}$$

For an element of fluid sized at *dx* in width and *h* in height, the equilibrium of forces acting on the element in *x* direction, lead to the following equation:

$$\frac{\partial \sigma_{xx}}{\partial x}h - \tau_{xy}\,|_{y=\frac{h}{2}} - \tau_{xy}\,|_{y=-\frac{h}{2}} = 0 \tag{10}$$

Using (9) in (10) results in:

$$\frac{\partial \sigma_{xx}}{\partial x} = 2^{n-1}\frac{mw}{w_0 h_0}\left(\frac{\dot{w}}{w}\right)^n\left(\frac{1}{\beta_t}+\frac{1}{\beta_b}\right)x \tag{11}$$

Where β_t and β_b denote slip lengths at top and bottom interfaces, respectively. By integration with respect to x and considering that $\sigma_{xx} = 0$ at $x = \frac{w}{2}, -\frac{w}{2}$, the normal stress distribution along x is:

$$\sigma_{xx} = 2^{n-2}\frac{m\, w^{1-n}\, \dot{w}^n}{w_0 h_0}\left(\frac{1}{\beta_t}+\frac{1}{\beta_b}\right)(x^2 - \frac{w^2}{4}) \tag{12}$$

Also, it is known that:

$$\sigma_{xx} = -p + 2^n m \dot{\varepsilon}_{xx}{}^{\mathrm{n}} \tag{13}$$

Furthermore:

$$\sigma_{yy} = -p - 2^n m \dot{\varepsilon}_{xx}{}^{\mathrm{n}} \tag{14}$$

By substituting (12) in (13) pressure can be found in terms of remaining parameters, and then using (14), the following relation is obtained for normal stress in y direction (Due to the dominance of elongational strain rate, elements of fluid experience similar strain rate and deformation, and therefore $\dot{\varepsilon}_{xx} = \frac{\dot{w}}{w}$):

$$\sigma_{yy} = 2^{n-2}\frac{m\, w^{1-n}\, \dot{w}^n}{w_0 h_0}\left(\frac{1}{\beta_t}+\frac{1}{\beta_b}\right)(x^2 - \frac{w^2}{4}) - 2^{n+1} m (\frac{\dot{w}}{w})^{\mathrm{n}} \tag{15}$$

Subsequently to calculate force per unit of z axis (unit of consolidation length):

$$q = \left|\int_{-\frac{w}{2}}^{\frac{w}{2}} \sigma_{yy}\, dx\right| = -2^{n-1}\frac{m\, w^{1-n}\, \dot{w}^n}{w_0 h_0}\left(\frac{1}{\beta_t}+\frac{1}{\beta_b}\right)\left(\frac{w^3}{24} - \frac{w^3}{8}\right) + 2^{n+2} m\left(\frac{\dot{w}}{w}\right)^{\mathrm{n}}\left(\frac{w}{2}\right) \tag{16}$$

By manipulating right side of equation, raising both side to the power of 1/n, and then integrating with respect to time:

$$\int_0^t q(\tau)^{1/n} d\tau = \int_{w_0}^{w_t}\left(2^{n-3}\frac{m\, w^{4-n}}{3 w_0 h_0}\left(\frac{1}{\beta_t}+\frac{1}{\beta_b}\right) + 2^{n+1} m\, w^{1-\mathrm{n}}\right)^{1/n} dw \tag{17}$$

There is no analytical antiderivative for right-side expression. However, an approximation can be made using two-term Binomial expansion for the simplification of right side, and assuming q constant across z for simplification of left side. The integration across the whole domain leads to:

$$if \;\; \frac{\beta_b \beta_t}{\beta_b + \beta_t} < \frac{w_0^2}{48\, h_0}: \qquad F^{\frac{1}{n}}\, l^{\frac{n-1}{n}}\, V^{-1} \approx b^{\frac{1}{n}}\left[\frac{n}{4}(w_f^{\frac{4}{n}} - w_0^{\frac{4}{n}}) + \frac{a}{-3n+4}(w_f^{-3+\frac{4}{n}} - w_0^{-3+\frac{4}{n}})\right] \tag{18}$$

$$if \;\; \frac{\beta_b \beta_t}{\beta_b + \beta_t} > \frac{w_0^2}{48\, h_0}: \qquad F^{\frac{1}{n}}\, l^{\frac{n-1}{n}}\, V^{-1} \approx (ab)^{\frac{1}{n}}[n\,(w_f^{\frac{1}{n}} - w_0^{\frac{1}{n}}) + \frac{1}{a(n+3)}(w_f^{\frac{1}{n}+3} - w_0^{\frac{1}{n}+3})] \tag{19}$$

Where:

$$a = 48\, w_0 h_0 \frac{\beta_b \beta_t}{\beta_b + \beta_t} \tag{20}$$

$$b = 2^{n-3} \frac{m}{3 w_0 h_0} \left(\frac{1}{\beta_t} + \frac{1}{\beta_b}\right) \tag{21}$$

Depending on the value of $\frac{\beta_b \beta_t}{\beta_b+\beta_t}$ (or $\frac{\beta_{eq}}{2}$,where β_{eq} is defined as equivalent slip length), either Equation 18 or 19 can be used for final width prediction. F, l , V, and w_f are compaction force, consolidation length (also known as contact length), layup velocity, and final width of consolidated tape, respectively. For a known w_f, an unknown process parameter can be obtained. Conversely, for known process parameters, obtaining a closed-form expression for w_f is not feasible. Nevertheless, employing straightforward iterations enables the determination of w_f .

3 RESULTS

The results obtained by the model are displayed in Figure 2 (material parameters listed in Table 1) and are compared against experimental measurements on samples made by hot-gas-torch AFP equipment (utilizing hard roller) on zero-degree composite substrate angle using AFP machine at Concordia University. Through a trial-and-error process, a suitable value of β_{eq} was simply identified to ensure a close fit between the theoretical curve and the experimental data. By only selecting a single scalar value for β_{eq}, both curves for two different temperatures demonstrated a satisfactory agreement with the experimental results. Moreover, as shown in the figure for the sake of comparison with other models, the well-known no slip (infinite friction; purely shear flow) or perfect slip (zero-friction; purely extensional flow) conditions are ineffective in capturing the squeezing flow of thin composite tape under rapid consolidation of compaction roller.

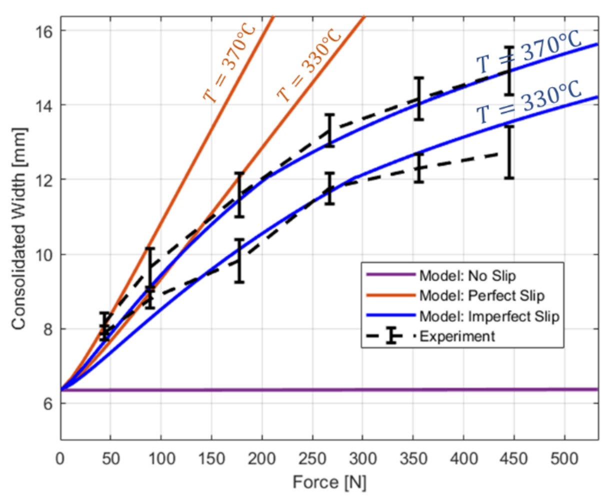

Figure 2. Final width of consolidated tape as a function of compaction force under two different temperatures: Comparison of Imperfect Slip Squeeze model (blue curves) and experimental data

Table 1. Material properties and dimensions.

Tape parameters	Values for analysis
m [Pa.s]	6.358 E5 (370 ℃) [6]
	8.525 E5 (330 ℃)
n [1]	0.65
w_0 [m]	6.35 E-3
h_0 [m]	1.5 E-4

4 CONCLUSION

This work aimed to develop a new squeeze flow model with incorporation of strong wall slippage for thermoplastic composite tapes in-situ consolidated via automated fiber placement. Power law viscosity expression has been used to develop constitutive equations for two-dimensional incompressible non-Newtonian fluid. While perfect slip (zero-friction; purely extensional flow) and no slip (infinite friction; purely shear flow) squeeze models fail to predict consolidated tape width, the presented imperfect slip squeeze model is capable of feasible predictions after extracting suitable value for slip length.

5 REFERENCES

[1] Fereidouni M, Hoa SV. In-situ consolidation of thermoplastic composites by automated fiber placement: Characterization of defects. Journal of Thermoplastic Composite Materials. 2024 May 8:08927057241251837.

[2] Agarwal S. Width deformation of thermoplastic prepreg tapes during in-situ automated fiber placement: an experimental investigation into the width deformation mechanism and influence of processing parameters. Master thesis. Delft University of Technology, September 2023

[3] Oromiehie E, Gain AK, Prusty BG. Processing parameter optimisation for automated fibre placement (AFP) manufactured thermoplastic composites. Composite Structures. 2021 Sep 15;272:114223.

[4] Reddy JN. An introduction to continuum mechanics. Cambridge university press; 2013 Jul 29.

[5] Navier CL. Memoires sur les lois du movement des fluides, Mem. Acad. Sci. Inst. France 6 (1822) 389.

[6] Shuler SF, Advani SG. Transverse squeeze flow of concentrated aligned fibers in viscous fluids. Journal of Non-Newtonian Fluid Mechanics. 1996 Jul 1;65(1):47-74.